Supplemental Figures and Legends (Lobo et al)

Supplemental Figure S1. Germline and Cancer-derived *PTEN* missense mutations occurring in the PTEN ATP-binding domain. The consensus Type-A ATP binding and Type-B ATP binding motifs within the N-terminal phosphatase domain of PTEN are underlined. The positions of cancer-associated *PTEN* mutations, previously identified by us, and occurring within the ATP-binding motifs on PTEN are indicated in bold and shaded in yellow, while *de novo* germline *PTEN* mutations occurring in Cowden syndrome patients are indicated in bold and highlighted in green.

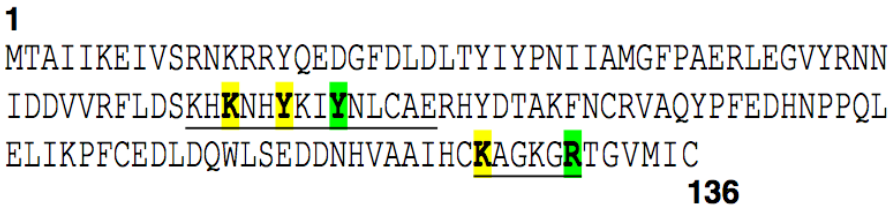

Supplementary Figure 1

Supplemental Figure S2. Germline *PTEN* mutations, derived from CS patients, have decreased ATP-binding.

Total protein from controls (*PTEN* mutation negative individuals) and from lymphoblastoid cell lines expressing mutant PTEN (from 4 Cowden syndrome patients) were subjected to ATP-binding assays and western analysis as described in methods. Wild-type PTEN from controls bound efficiently to ATP. In contrast, mutant protein from the 4 CS patients showed decreased ATP-binding.

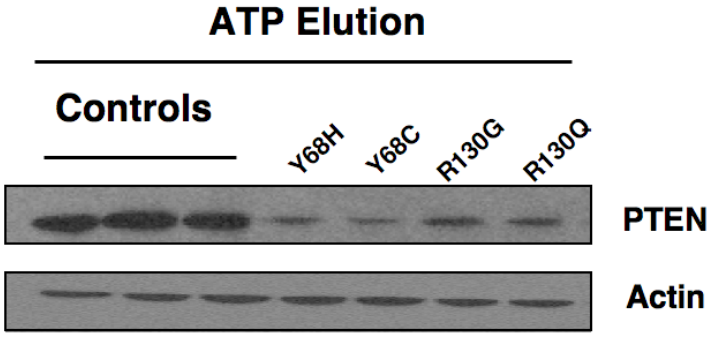

Supplementary Figure 2

Supplemental Figure S3. Cancer-associated somatic missense mutations in the ATP-binding domain of PTEN favor its nuclear localization, in cell lines other than those shown for Figure 1.

Cells were transfected with either wild-type PTEN or individual PTEN mutants, as indicated. Exogenously expressed PTEN was detected by direct immunofluorescence using an α-FLAG M2 FITC conjugated antibody. PTEN expression is detected as green fluorescence. Nuclei were also concurrently stained with DAPI, which was included in the mounting medium. Representative images showing the localization of wild-type PTEN and each cancer-derived mutant PTEN are shown. Over-expressed wild-type PTEN localizes both to the cytoplasm and nucleus in all cell types assayed. The K62R- and Y65C- PTEN mutants (within the Type-B ATP binding sites) and the K125E PTEN mutant (within the Type A-ATP binding sites) localize predominantly to the nucleus, and are morphologically different in all cell types analyzed. **A**) MDA-MB-231, breast carcinoma cells. **B**) WM164, melanoma cell line. **C**) RKO, colorectal carcinoma cell line. All experiments were carried out in duplicate. Approximately 100 cells were counted per individual transfection and representative images from three separate experiments are shown. All images were acquired at 40x magnification.

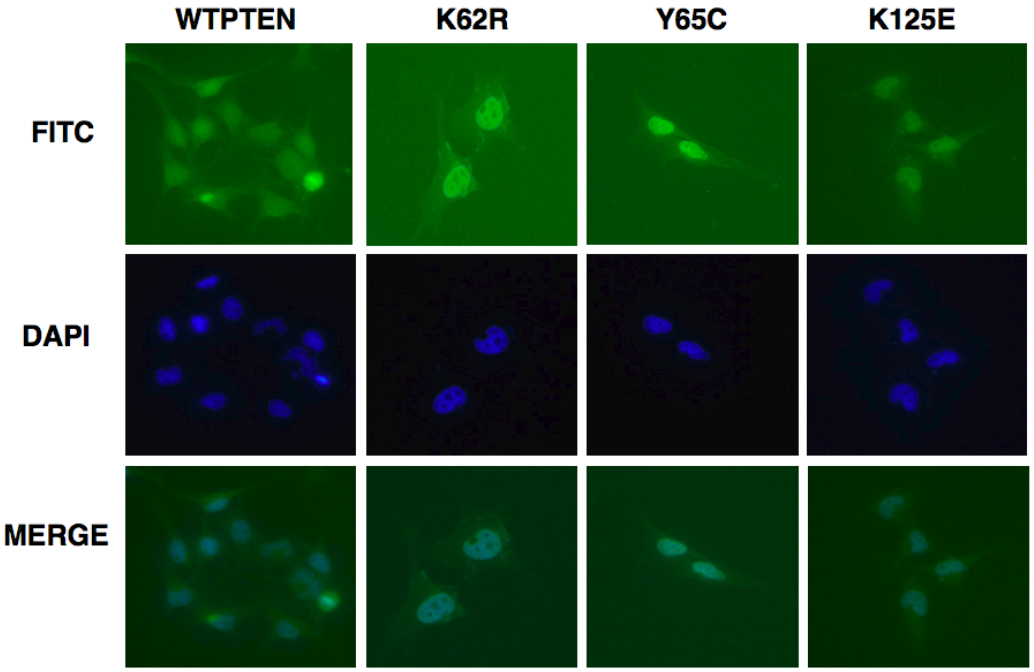

Supplementary Figure 3A

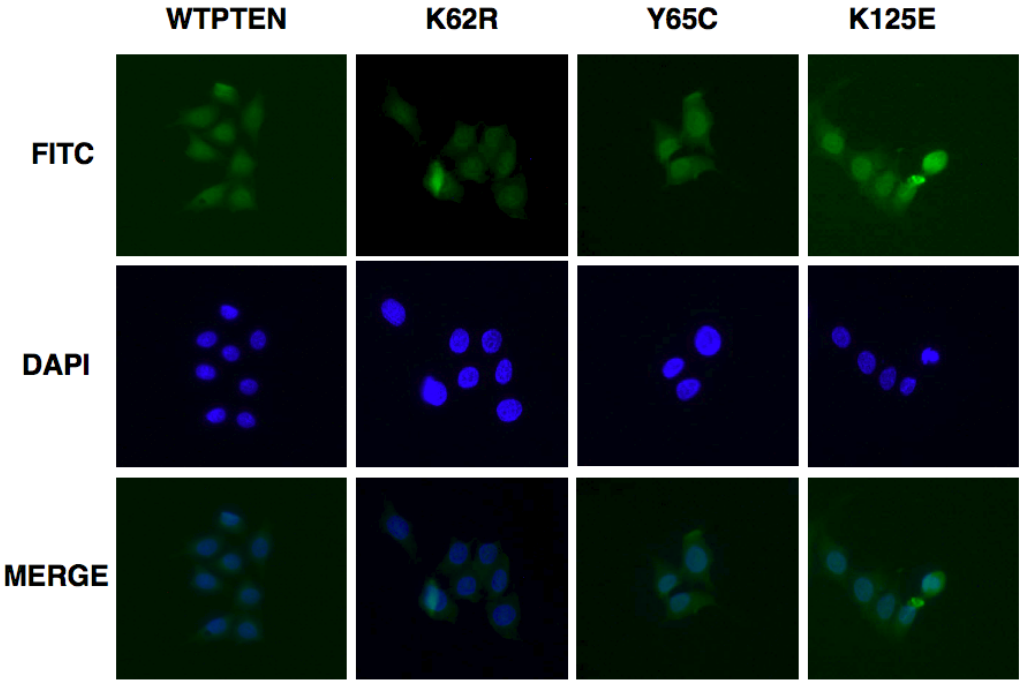

Supplementary Figure 3B

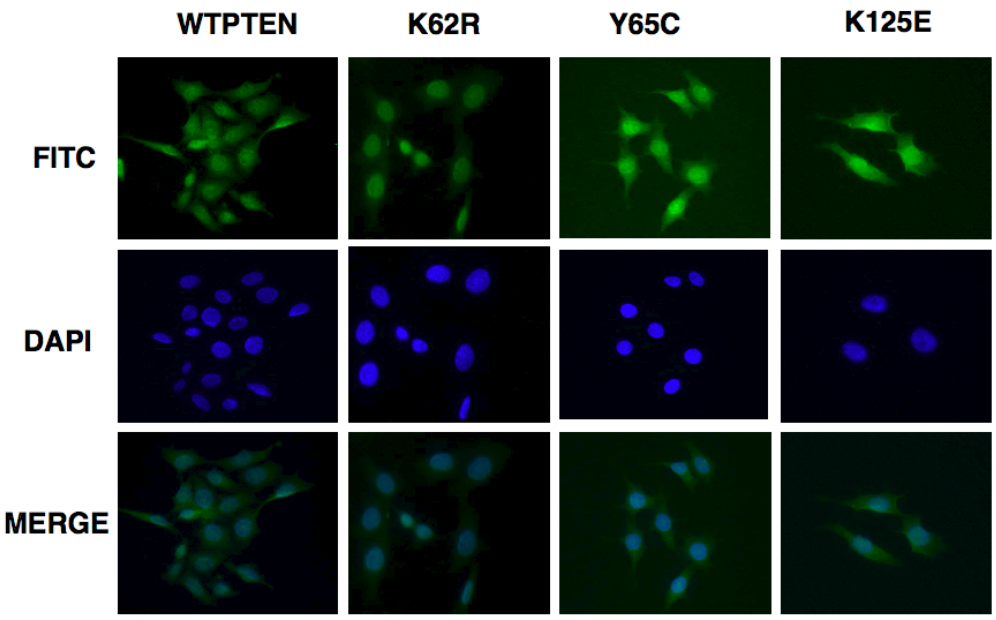

Supplementary Figure 3C

Supplemental Figure S4. Multiple sequence alignment of PTEN from diverse species. Multiple sequence alignment of exon 3 and 5 of PTEN protein from diverse species is shown. Germline (highlighted in red) and cancer-associated *PTEN* mutations within the N-terminal PTEN ATP-binding sites are indicated in bold. The amino acid codon(s) conserved between the diverse species is highlighted in yellow.

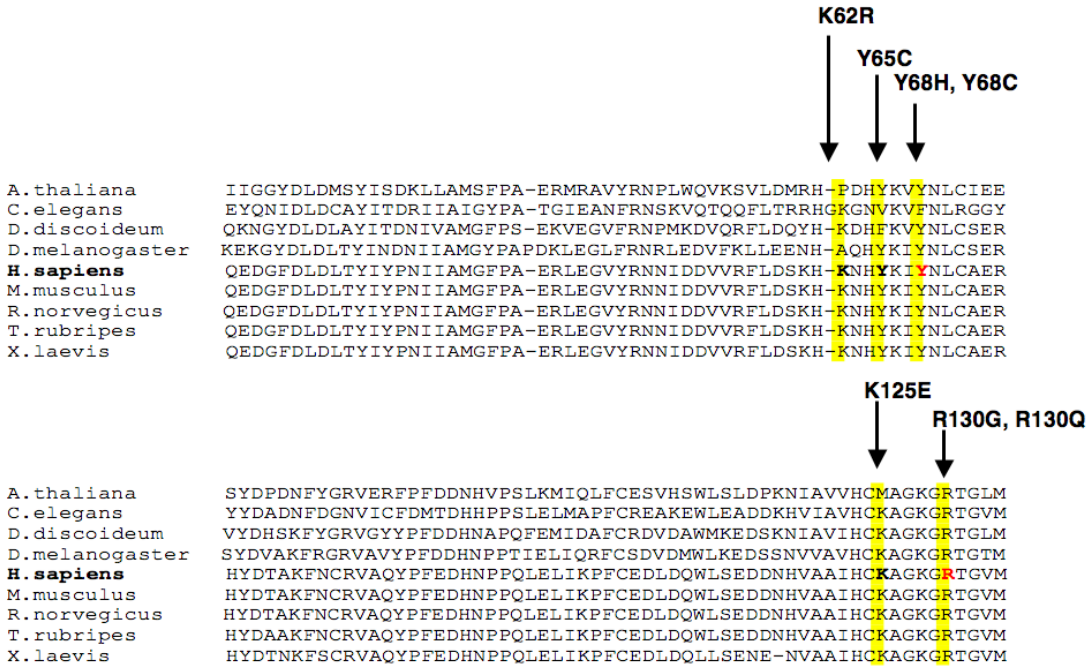

Supplementary Figure 4

Supplemental Figure S5. *PTEN* missense mutations outside the ATP-binding motifs do not alter nuclear (N):cytoplasmic (C) PTEN expression.

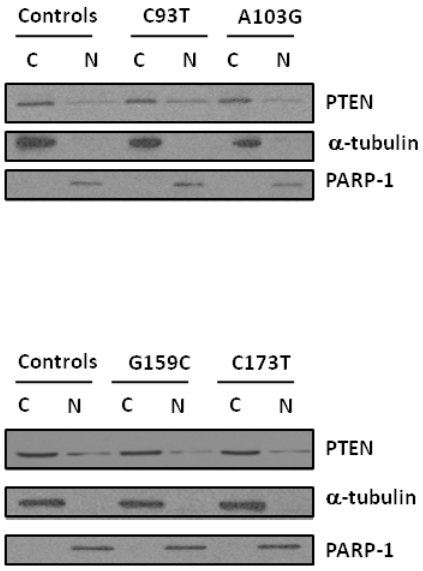

Supplemental Figure S6. Germline *PTEN* missense mutations, derived from CS patients, that do not involve the ATP-binding regions do not have decreased ATP-binding.

Total protein from controls (*PTEN* mutation negative individuals) and from lymphoblastoid cell lines expressing mutant PTEN (from 4 Cowden syndrome patients) were subjected to ATP-binding assays and western analysis as described in methods. Both wild-type PTEN from controls as well as non-ATP-binding missense mutant PTEN bound efficiently to ATP.

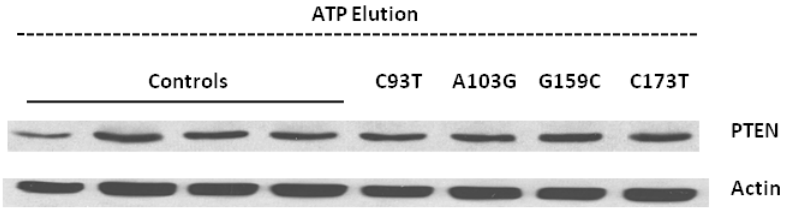

Supplemental Figure S7. Charge neutral mutants K62Q-, Y65Q- and the K125Q-PTEN show nuclear mislocalization compared to controls but the effect is decreased compared to the K62R- and Y65C- PTEN mutants (within the Type-B ATP binding sites) and the K125E (Type-B ATP binding site) [compare to Fig. 1A].